

## Supporting Information For

### **Antitumor Activity and Molecular Dynamics Simulations of Paclitaxel-Laden Triazine Dendrimer**

Jongdoo Lim,<sup>†,1</sup> Su-Tang Lo,<sup>‡,1</sup> Sonia Hill,<sup>‡</sup> Giovanni M. Pavan,<sup>¶,\*</sup> Xiankai Sun,<sup>‡,\*</sup> Eric E. Simanek<sup>†,\*</sup>

#### Table of Contents

Figure S1. Tumor Volume Ratios of Therapeutic Efficacy	2
Figure S2. Blood cell counting in WBCs, RBCs, and platelets	3
Figure S3. Change of whole body weight	4
Figure S4. Biodistribution studies	5
Note on Computation	6

**Figure S1.** Therapeutic efficacy of prodrug **2** in SCID mice with PC3-h-luc xenografts. The tumor size change was estimated using calipers during the study of 60-day.

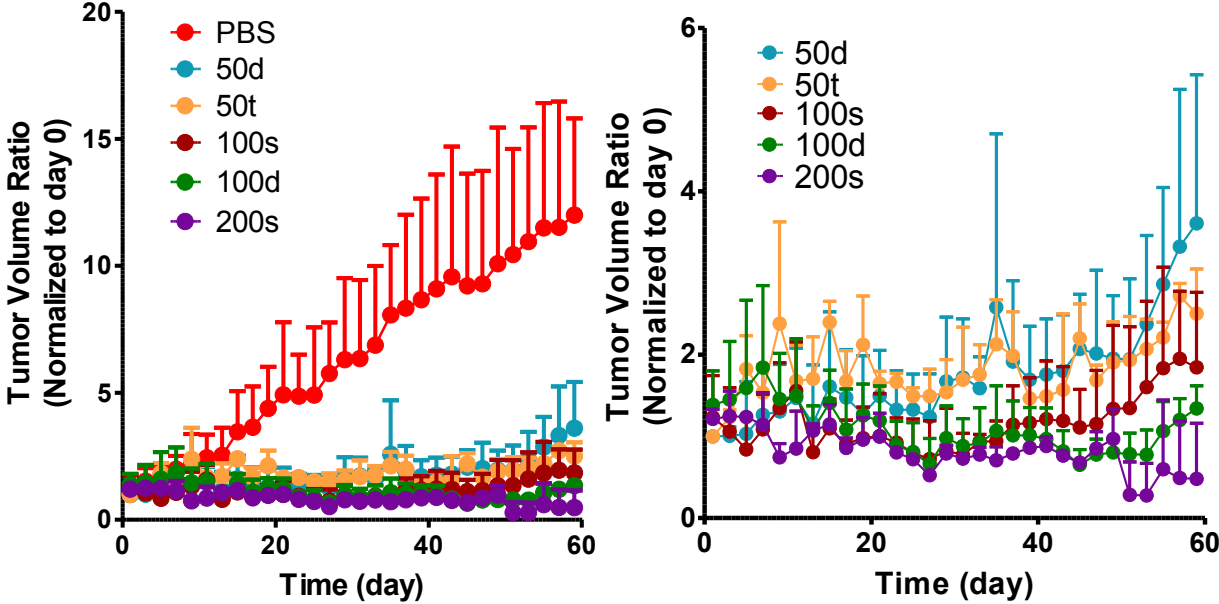


**Figure S2.** Blood cell counting in WBCs, RBCs, and platelets obtained from mice treated with **2-50d**, **2-50t** or PBS.

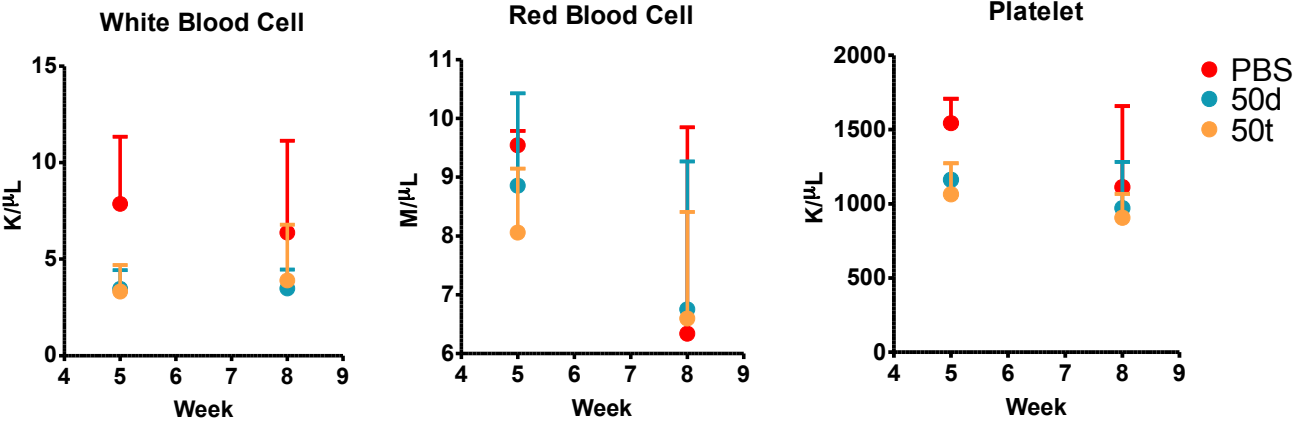
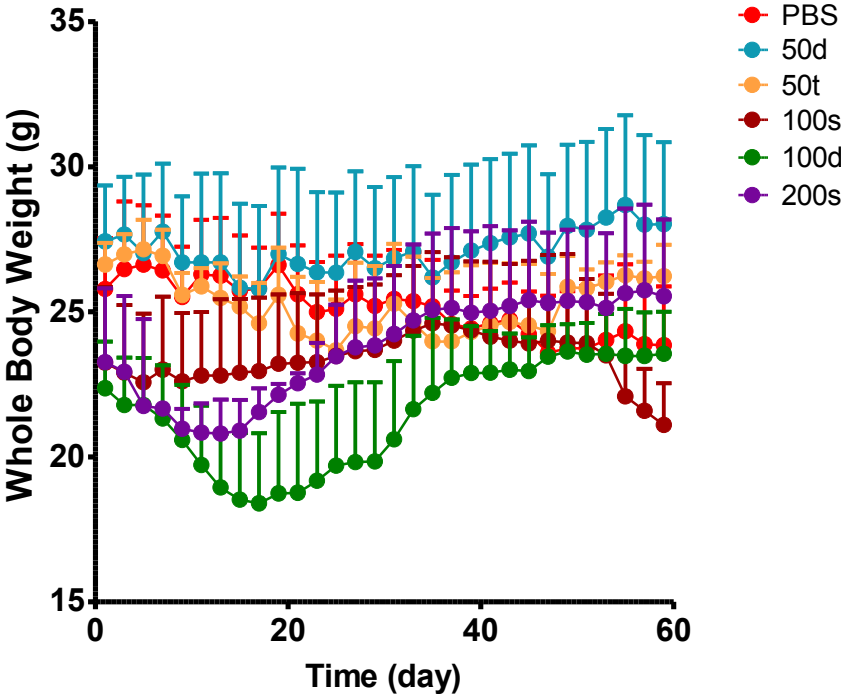
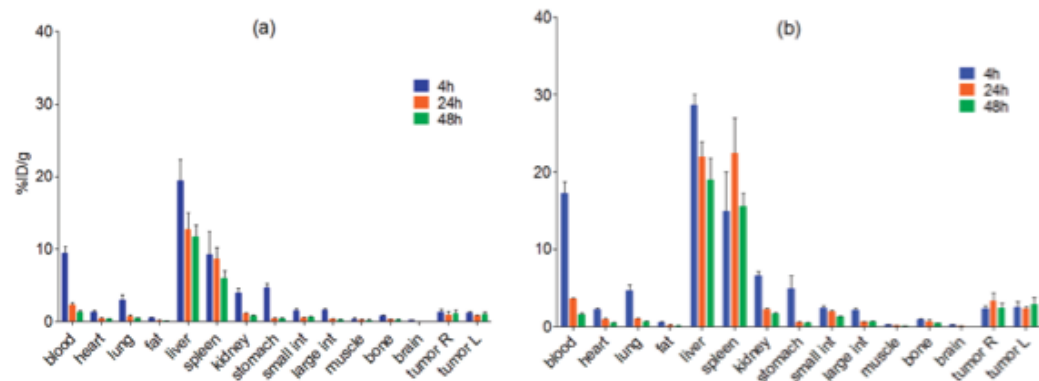


Figure S3. Change in whole body weight over the course of the experiment.



**Figure S4.** Biodistribution studies of **1** and **2**.



**A note on computational studies.** Paclitaxel has been the subject of multiple computational studies. For a representative example of computation applied to the solution conformation of paclitaxel, see:

"Solution structure of taxol determined using a novel feedback-scaling procedure for NOE-restrained molecular dynamics." R.E. Cachau, R. Gussio, J.A. Beutler, G.N. Chmurny, B.D. Hilton, G.M. Muschik, and J.W. Erickson, *The International Journal of Supercomputer Applications and High Performance Computing* (MIT Press Journals), 8(1), 24-34 (1994).

### Distribution of Ester Linkages and the Role of PEG.

When the RDF plots are normalized to reflect, by area, the same number of paclitaxel groups, an interesting picture emerges. A similar distribution of all 12 ester-groups is observed across the hexaPEGylated, nonaPEGylated, and dodecaPEGylated materials. To calculate this distribution, spheres of radius 1 Å were created starting at the center, and the number of esters inside the sphere were counted. By comparing this distribution with the observed  $R_g$ , we can conclude that the majority of esters are close to the surface. All dendrimers have at least one ester backfolded at distance  $<10$  Å from the center, and 2 at  $<20$  Å. This backfolding is represented by the first peak at  $\sim 10$  Å in the plots of Figure S5. Overlaying these plots as shown in Figure S6 A, or by counting esters as a function of distance (Figure S6 B), we conclude that the esters are all similarly distributed. This distribution is close to the surface of the dendrimer, as revealed by the coincidental value of  $\sim 24$  Å of both the numeric plot and the calculated radii of gyration (Figure S7) for all these species. In conclusion, computation does not afford a clear compulsion for fractionation.

**Figure S5.** Radial distribution functions of hexaPEGylated (A), nonaPEGylated (B), and dodecaPEGylated (C) constructs where both the PTX 2' ester group and PEGs are quantified.

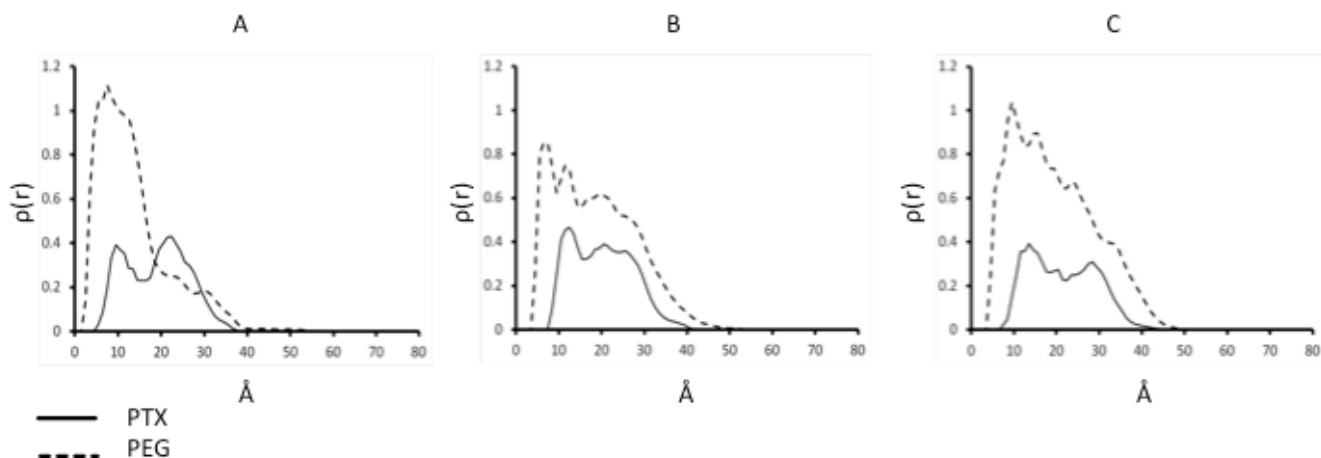


**Figure S6.** Combined RDFs (A) or integer plots (B) for the hexaPEGylated (solid), nonPEGylated (dashed), and dodecaPEGylated (dotted) constructs showing similar distributions of ester linkages.

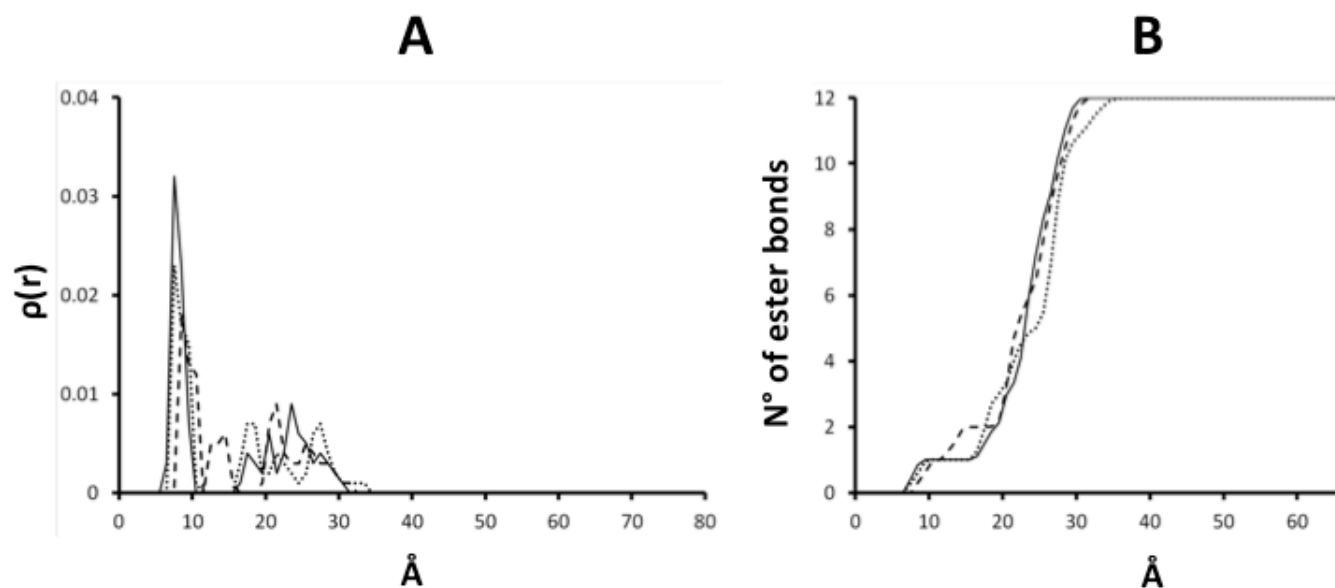


**Figure S7.** Radii of gyration from computation for the constructs in 150mM saline.

### Radius of gyration in 150 mM salt solution

